HOKKAIDO UNIVERSITY

Title	All-solid-state electrochemical capacitors using MnO2/carbon nanotube composite electrode
Author(s)	Shimamoto, Kazushi; Tadanaga, Kiyoharu; Tatsumisago, Masahiro
Citation	Electrochimica acta, 109, 651-655 https://doi.org/10.1016/j.electacta.2013.07.154
Issue Date	2013-10-30
Doc URL	https://hdl.handle.net/2115/57394
Type	journal article
File Information	capaciter-shimamoto-accepte.pdf

Hokkaido University Collection of Scholarly and Academic Papers : HUSCAP

All-Solid-State Electrochemical Capacitors Using MnO_2/Carbon Nanotube Composite Electrode

Kazushi Shimamoto, Kiyoharu Tadanaga*, and Masahiro Tatsumisago

Department of Applied Chemistry, Graduate School of Engineering,

Osaka Prefecture University, 1-1 Gakuen-cho, Naka-ku, Sakai, Osaka 599-8531, Japan

Corresponding author
Kiyoharu Tadanaga
Present address
Faculty of Engineering, Hokkaido University
Sapporo, Hokkaido 060-8628, Japan
E-mail: tadanaga@eng.hokudai.ac.jp

Abstract

MnO_2/carbon nanotube (CNT) composite was prepared by a solution process. In the obtained MnO_2-CNT composite, MnO_2 particles were well-dispersed on CNTs. The specific capacitance of the MnO_2-CNT composite in an aqueous electrolyte was higher than that of MnO_2 and CNT. All-solid-state electrochemical capacitors (ECs) were fabricated using the MnO_2-CNT composite as a positive electrode, activated carbon powder as a negative electrode, and phosphosilicate gel as an electrolyte. The obtained all-solid-state ECs operated at the temperature range between -30°C and 100°C. The specific discharge capacitance and the rate ability of the capacitors were improved by elevating temperature. In addition, the fabricated all-solid-state ECs exhibited excellent cycle performance at the temperature range between -30°C and 100°C for 20,000 cycles. These results indicate that all-solid-state ECs using MnO_2 are promising energy storage devices with excellent stability and high reliability at the wide range of temperatures.

Keywords

Manganese oxides, Carbon nanotube, All-solid-state capacitor, Solid electrolyte, Phosphosilicate gel,

1. Introduction

Electrochemical capacitors (ECs) are one of the most promising energy storage devices because of their high power density, fast charge-discharge, and good cycle performance [1-3]. In recent years, transition metal oxides which store energy by utilizing the pseudocapacitance arising from fast and reversible faradic reactions in the electrode surface are good fundamental candidates for ECs [4-6]. Among the various metal oxides, ruthenium oxide (RuO_2) is widely studied because of its high specific capacitance (~720 F g^{-1}) [7, 8]. However, the commercial use of RuO_2 will be limited because of its high cost. Therefore, alternative and inexpensive electrode materials have been explored.

Manganese dioxide (MnO_2) is a good candidate material for the active electrode material due to its low cost, abundance, high theoretical specific capacitance (~1100 F g^{-1}) and environmentally-friendliness [9-11]. MnO_2 is often prepared using a solution process to obtain the large specific surface area [12-14]. However, the electron conductivity of MnO_2 is not high enough to use it as an electrode material for ECs. In order to realize an excellent electrode with MnO_2, the formation of good electron conductive paths is important. Carbon nanotube (CNT) has recently been paid attention to its high electron conductivity and good chemical stability [15]. It has been

demonstrated that CNT noticeably enhances the electrical properties of composite materials [16]. Thus, CNT can be used as the good electrical conducting material to form the electron conductive paths of MnO_2. In fact, MnO_2-CNT composite have been studied for ECs [16].

MnO_2 electrodes often operates in aqueous solution electrolytes such as KCl aq. and Na_2SO_4 aq. [9-14]. However, the use of these aqueous solution electrolytes has several problems such as electrolyte leakage, solvent corrosion, packing difficulty, and dissolution of MnO_2 at charge-discharge process [17, 18]. To overcome these issues, ECs using solid electrolyte have been proposed [19-22]. All-solid-state ECs is expected to have a high safety and reliability because of non-leakage and wide range of operating temperature. Thus, all-solid-state ECs have been studied in recent years. For example, Yuan et al. fabricated all-solid-state ECs using MnO_2 as electrodes and PVA-H_3PO_4 as an electrolyte [19]. Organic polymers are often used as electrolytes of all-solid-state ECs [19-22]. However, organic polymer electrolytes generally show a low thermal stability and a large humidity dependence of ion conductivity. Therefore, stable solid electrolytes at the various ranges of temperature and humidity have been required.

Among various types of alternative solid electrolytes, phosphoric acid doped silica

gel called as phosphosilicate gel is a good candidate electrolyte due to its good thermal stability and humidity independent performance [23, 24]. The phosphosilicate gel shows a high ion conductivity of about 10^{-3} S cm^{-1} in a dry atmosphere at room temperature and keep a high ion conductivity even after holding for 6 h under 0.7% relative humidity at 130°C [23, 24]. We have already fabricated all-solid-state electric double layer capacitors using phosphoric acid-doped silica gel as an electrolyte and carbon materials as polarized electrodes [25, 26]. By using MnO_2 as an electrode, the all-solid-state ECs are expected to show higher specific capacitance and energy density than the all-solid-state electric double-layer capacitors.

In this study, a MnO_2-CNT composite electrode was prepared by a solution process. The MnO_2-CNT composite was formed from a precursor solution of MnO_2 containing CNT to form a good contact between MnO_2 and CNT. The microstructure and electrochemical properties of the obtained MnO_2-CNT composite electrode were examined. Then, all-solid-state ECs using the MnO_2-CNT composite as a positive electrode, activated carbon powder (ACP) as a negative electrode, and phosphosilicate gel as an electrolyte were fabricated. An electrode using the MnO_2-CNT composite was first applied to all-solid-state ECs. The electrochemical properties of the ECs were studied in a temperature range of -30°C to 100°C.

2. Experimental

2.1. Preparation and characterization of MnO_2-CNT composite

A MnO_2-CNT composite was prepared by using a solution process. $MnSO_4 \cdot 5H_2O$ and polyoxyethylene(7) oleyl ether as a surfactant agent were added into distilled water. CNT (Aldrich, >90% carbon basis) was added (15 wt% in the final composite) to the mixed solution. The mixed solution was stirred for 6 h to disperse CNT in the solution. Then, $KMnO_4$ dissolved aqueous solution was added drop by drop into the mixed solution. The molar ratio of $MnSO_4$:$KMnO_4$:polyoxyethylene(7) oleyl ether was fixed to be 1:1:0.1. The resulting black precipitates were filtrated, washed with distilled water and ethanol, and dried at 80 ^oC for 1 day.

The as-prepared MnO_2-CNT composite was characterized using X-ray diffraction measurements (Cu Kα) and scanning electron microscope (SEM, JED-2300, JEOL). The specific surface area of the MnO_2-CNT composite was determined by the Brunauer-Emmett-Teller (BET) technique with N_2 gas. The electronic conductivity of the MnO_2-CNT composite was investigated by a DC polarization technique.

The electrochemical characterization of the MnO_2-CNT composite was performed using a half cell in a liquid electrolyte. The as-prepared MnO_2-CNT composite, MnO_2, or CNT (95 wt%) as an active material, poly(tetrafluoroethylene) (5 wt%) as a binder

and distilled water as a solvent were mixed and pasted onto a nickel foam substrate (1 cm × 1 cm) with a spatula, which was followed by drying at 80°C for 3 h. Cyclic voltammetry (CV, HSV-100, Hokuto Denkou) was measured in a three-electrode setup : a nickel foam coated with MnO_2-CNT composite, MnO_2, and CNT as the working electrodes, a platinum plate as the counter electrode, Ag/AgCl saturated KCl as the reference electrode, and 0.5 M Na_2SO_4 aqueous solution as the electrolyte.

2.2. Preparation of phosphosilicate gel and negative electrode

Phosphosilicate gel was prepared by the sol-gel method. Tetraethoxysilane (TEOS) was diluted with ethanol and hydrolyzed with H_2O containing HCl with stirring at room temperature for 10 min. An appropriate amount of phosphoric acid was added to the hydrolyzed solution and then stirred at room temperature for 3 h. The mole ratio of TEOS:ethanol:H_2O:HCl:phosphoric acid was fixed to be 1:8:4:0.01:1. The obtained phosphosilicate sol was kept at 50°C in a closed vessel to form wet phosphosilicate gel. The wet gel was dried at 50°C for an additional 1 week in an open vessel. The dry gel, which was pulverized into powders with an agate mortar and a pestle, was heat-treated at 150°C for 5 h. The electrical conductivities of the phosphosilicate gel were measured using AC impedance data (10^6 Hz~0.1 Hz, Solartron 1260; Solartron).

For the preparation of the negative electrode, ACP (specific surface area of ca. 1100 m^2g^{-1}, Kanto Kagaku) and Acetylene Black (AB, Aldrich) were add in the phosphosilicate sols. The weight ratio of phosphosilicate sol:ACP:AB was fixed to be 15:1:0.15. The mixed sol was stirred until gelation. The wet gel was dried at 50°C for an additional 1 week. The obtained ACP-AB-phosphosilicate gel composite was heat-treated at 150°C for 5 h.

2.3. Fabrication of all-solid-state ECs

The all-solid-state ECs were fabricated using the mixture of MnO_2-CNT composite, AB (to fabricate electron conduction paths), and phosphosilicate gel (to fabricate ion conduction path) as the positive electrode, ACP-AB-phosphosilicate gel composite as the negative electrode and phosphosilicate gel as the solid electrolyte. The powders of positive electrode, the solid electrolyte, and the negative electrode were placed in a polycarbonate tube (ϕ =10 mm) and pressed under 360 MPa. Then the three-layered pellet was sandwiched by two stainless-steel rods as current collectors. The weight ratio of positive active material (MnO_2-CNT composite):negative active material (ACP) was fixed to be 1:2. The as-prepared all-solid-state ECs were characterized by CV measurement and charge-discharge test at -30°C, 25°C, and 100°C. The

charge-discharge test was performed using a charge-discharge measuring device (BTS-2004, Nagao Co.).

3. Results and discussion

3.1. Characterization of MnO_2-CNT composite

Figure 1 shows the X-ray diffraction patterns of (a)MnO_2, (b)CNT, and (C) MnO_2-CNT composite. X-ray diffraction analysis of the MnO_2-CNT composite confirmed the presence of CNT and α-MnO_2 (JCPDS 44-0141). Two broad peaks around 24^o and 37^o can be indexed to α-MnO_2 phase, corresponding to (220) and (211) planes. Figure 2 shows the SEM images of (a)MnO_2, (b)CNT, and (c)MnO_2-CNT composite. MnO_2 is spherical particles with a diameter of about 1 μm (Fig. 2a) and the CNT used in the present study exhibits regular morphology with a diameter of about 100~200 nm (Fig. 2b). The as-prepared MnO_2-CNT composite exhibits complexly intertwined MnO_2 particles and CNTs. This morphology suggests that good electron conductive paths are formed in the composite. BET surface area analysis showed that a specific surface area of MnO_2 was 138 m^2g^{-1}, CNT 9 m^2g^{-1}, and the MnO_2-CNT composite 83 m^2g^{-1}.

Figure 3 exhibits the cyclic voltammograms of the electrode with (a)MnO_2,

(b)CNT, and (c)MnO_2-CNT composite between 0 and 1.0 V (vs. Ag/AgCl) in 0.5 M Na_2SO_4 aqueous solution at the scan rate of 5 mV s^{-1}. The cyclic voltammograms of the MnO_2 electrode and the MnO_2-CNT composite electrode show rectangular profiles, indicating that the MnO_2 electrode and the MnO_2-CNT electrode have ideal capacitive behaviors. The specific capacitance is calculated using from the voltammogram the following equation(1):

$$Cs = \int \frac{i}{\Delta V\, m}\, dt = \int \frac{i}{\Delta V\, m}\, dV \left(\frac{dt}{dV}\right) = \int \frac{i}{\Delta V\, m\, a}\, dV \qquad (1)$$

where *Cs* is the specific capacitance, i is the discharge current, ΔV is the voltage range, *m* is the total mass of electrode and *a* is the scan rate. The specific capacitances of the MnO_2, CNT, and MnO_2-CNT composite are 50, 3, and 215 Fg^{-1}, respectively, at the scan rate of 5 mV s^{-1}. CNT is a very low specific capacitance because of its small specific surface area (9 m^2 g^{-1}). Although the MnO_2-CNT composite has smaller specific surface area (83 m^2 g^{-1}) than MnO_2 (138 m^2 g^{-1}), the MnO_2-CNT composite has approximately four times larger specific capacitance than MnO_2. These results suggest that MnO_2-CNT composite forms good electron conductive paths by complexly intertwined MnO_2 particles and CNT. Hence, the introduction of MnO_2 as well-dispersed on CNT can effectively promote the electrochemical performance to increase the pseudo-capacitance of MnO_2.

3.2. Fabrication and characterization of all-solid-state ECs

All-solid-state ECs were fabricated using MnO_2-CNT as the positive electrode, ACP as the negative electrode, and phosphosilicate gel as the electrolyte, respectively. The operation temperatures of all-solid-state ECs are -30°C, 25°C, and 100°C. The ionic conductivity of the phosphosilicate gel was 9.3×10^{-4} S cm^{-1} at -30°C, 5.1×10^{-3} S cm^{-1} at 25°C, and 1.4×10^{-2} S cm^{-1} at 100°C. Figure 4 exhibits the cyclic voltammograms of the all-solid-state ECs at -30°C, 25°C, and 100°C with the scan rate of 50 mV s^{-1}. The operating voltage for the all-solid-state ECs is in the range of 0-0.9 V. The fabricated all-solid-state ECs show ideal capacitive behaviors with nearly rectangular curves, showing that the fabricated all-solid-state ECs can be operated at the temperature range of between -30°C and 100°C. Redox peaks are observed at the cell voltage of 0.7 V and 0.4V in CV at 100°C, indicating that the ionic conductivity of the phosphosilicate gel increases with an increase in the temperature and the redox reaction of MnO_2 expressed as the equation (2) is promoted [11].

$$MnO_2 + H^+ + e- \rightleftharpoons MnOOH \quad (2)$$

Figure 5 exhibits the galvanostatic charge-discharge curves of the all-solid-state ECs at the operation temperatures of -30°C, 25°C, and 100°C with a current density of 1 mA cm^{-2}. The fabricated all-solid-state ECs show the typical triangular-shaped

and nearly linear galvanostatic charge-discharge curves at -30°C, 25°C, and 100°C. The charge-discharge time for the all-solid-state ECs is increased with an increase in temperature. These results correspond to the increase in the ion conductivity with temperature. Figure 6 shows the specific discharge capacitances as a function of discharge current density for the all-solid-state ECs. The specific discharge capacitance of the all-solid-state ECs was evaluated from each discharge curves using the following equation (3):

$$C = \frac{i\,\Delta t}{\Delta V\, m} \qquad (3)$$

where C is the specific discharge capacitance, i the discharge current, Δt the time for discharge, ΔV the cell voltage difference during discharge, and m the mass of active material. The specific discharge capacitances of the all-solid-state ECs at 1 mA cm^{-1} are calculated to be 63 F g^{-1} at 100°C, 33 F g^{-1} at 25°C, and 15 F g^{-1} at -30°C based on the total mass of active materials in the two electrodes. The capacitance retention ratios of the all-solid-state ECs at 50 mA cm^{-1} are 43% at 100°C, 24% at 25°C, and 13% at -30°C. These results are explained by the enhancement of the ion conductivity of phosphosilicate gel by elevating temperature. Therefore, the ionic conductivity of the phosphosilicate gel affects the specific discharge capacitance and rate performance of the all-solid-state ECs.

In the ECs of Carbon/MnO_2 with liquid electrolytes, specific discharge capacitances are reported to be about 40~50 F g^{-1} at room temperature [27-29]. Therefore, the all-solid state ECs have rather low specific discharge capacitances compared with a liquid electrolyte system. This result is due to the smaller contact area of the electrode active material and the solid electrolyte in the all-solid-state ECs. For the further improvement of the all-solid-state ECs performance, formation of favorable contact between an electrode active material and solid electrolyte is very important.

Figure 7 exhibits the cycle performance of the all-solid-state ECs at the operation temperature of -30°C, 25°C, and 100°C. The cycle performance of the all-solid-state ECs shows capacitance retention of 83% at -30°C, 87% at 25°C, and 85% at 100°C for 20000 cycles, demonstrating their excellent long-term cycle stability at various temperatures. Manganese oxides are known to show gradual dissolution into liquid electrolyte during charge-discharge cycles, and the cell performance is degraded [18, 30-32]. However, the present study proves that the use of an inorganic solid electrolyte is effective to suppress the dissolution of manganese oxides, especially in high temperature ranges.

4. Conclusion

MnO_2-CNT composite was prepared by a solution process. In the MnO_2-CNT composite, MnO_2 particles were well-dispersed on CNTs. Specific capacitance of the MnO_2-CNT composite electrode was larger than that of the MnO_2 or CNT electrode in Na_2SO_4 aqueous electrolyte because of the formation of good electron conductive paths by complexly intertwined MnO_2 particles and CNT. All-solid-state ECs were fabricated using MnO_2-CNT composite as the positive electrode, ACP as the negative electrode, and phosphosilicate gel as the electrolyte, respectively. Cyclic voltammetry and galvanostatic charge-discharge measurements demonstrated that the fabricated all-solid-state ECs operated at the temperature range of between -30°C and 100°C. The improvement of the specific discharge capacitance and rate performance was observed by elevating temperature. It is considered that this improvement of the cell performance is affected by the enhancement of ion conductivity of phosphosilicate gel by elevating temperature. The all-solid-state ECs showed excellent cycle stability for 20,000 cycles at -30°C, 25°C, and 100°C. Thus, we concluded that the all-solid-state ECs using MnO_2 have the great potential for the electronic device applications because of their excellent stability and high reliability in the wide range of temperatures.

References

[1] B. G. Choi, S. J. Chang, H.-W. Kang, C. P. Park, H. J. Kim, W. H. Hong, S.G. Lee, and Y. S. Huh, High performance of a solid-state flexible asymmetric supercapacitor based on graphene films, *Nanoscale*, **4** (2012) 4983-4988.

[2] R. Kotz and M. Cerlen, Principles and app;ications of electrochemical capacitors, *Electrochim. Acta*, **45** (2000) 2483-2498.

[3] D. Qu and H. Shi, Studies of activated carbons used in double layer capacitors, *J. Power Sources,* **74** (1998) 99-107.

[4] P. Simon and Y. Gogotsi, Materials for electrochemical capacitors, *Nat. Mater.,* **7** (2008) 845-854.

[5] J. Yan, Z. Fan, T. Wei, J. Cheng, B. Shao, K. Wang, L. Song, and M. Zhang, Carbon nanotube/MnO_2 composites synthesized by microwave-assisted method for supercapacitors with high power and energy density, *J. Power Sources*, **194** (2009) 1201-1207.

[6] H. Y. Lee and J.B. Goodenough, Supercapacitor behavior with KCl electrolyte, *J. Solid State Chem.*, **144** (1999) 220-223.

[7] J.H.Park, J. M. Ko, and O. O. Park, Carbon nanotube/RuO2 nanocomposite

electrodes for supercapacitors, *J. Electrochem. Soc*., **150** (2003) A864-A867.

[8] T. R. Jow, and J. P. Zheng, Electrochemical capacitors using hydrous ruthenium oxide and hydrogen inserted ruthenium oxide, *J. Electrochem. Soc*., **145** (1998) 49-52.

[9] W. Wei, X. Cui, W. Chen, and D. G. Ivey, Manganese oxide-based materials as electrochemical supercapacitor electrodes, *Chem.Soc.Rev.*, **40** (2011) 1697-1721.

[10] Y.-T. Wang, A.-H. Lu, H.-L. Zhang, and W.-C. Li, Synthesis of Nanostructured mesoporous manganese oxides with three-dimensional frameworks and their application in supercapacitors, *J. Phys.Chem.C*, **115** (2011) 5413-5421.

[11] M. Toupin, T. Brousse, and D. Bélanger, Charge storage mechanism of MnO_2 electrode used in aqueous electrochemical capacitor, *Chem. Mater.*, **16** (2004) 3184-3190.

[12] V. Subramanian, H. Zhu, R. Vajtai, P. M. Ajayan, and B. Wei, Hydrothermal synthesis and pseudocapacitance properties of MnO_2 nanostructures, *J. Phys. Chem. B*, **109** (2005) 20207-20214.

[13] X. Wang, X. Wang, W. Huang, P. J. Sebastian, and S. Gamboa, Sol-gel template synthesis of highly ordered MnO_2 nanowire arrays, *J. Power Sources*, **140** (2005) 211-215.

[14] Y. U. Jeong and A. Manthiram, Nanocrystalline manganese oxides for electrochemical capacitors with neutral electrolytes, *J. Electrochem. Soc.*, **149** (2002) A1419-A1422.

[15] A. L. M. Reddy and S. Ramaprabhu, Nanocrystalline metal oxides dispersed multiwalled carbon nanotubes as supercapacitor electrodes, *J. Phys. Chem. C*, **111** (2007) 7727-7734.

[16] E. Raymundo-Pinero, V. Khomenko, E. Frackowiak, and F. Beguin, Performance of manganese oxide/CNTs composites as electrode materials for electrochemical capacitors, *J. Electrochem. Soc.*, **152** (2005) A229-A235.

[17] D. Rathod, M. Vijay, N. Islam, R. Kannan, U. Kharul, S. Kurungot, and V. Pillai, Design of an “all solid-state” supercapacitor based on phosphoric acid doped polybenzimidazole (PBI) electrolyte, *J. Appl. Electrochem*, **39** (2009) 1097-1103.

[18] V. Khomenko, E. Raymundo-Pinero, and F. Beguin, Optimisation of an asymmetric manganese oxide/activated carbon capacitor working at 2 V in aqueous medium, *J. Power Sources*, **153** (2006) 183-190.

[19] L. Yuan, X.-H. Lu, X. Xiao, T. Zhai, J. Dai, F. Zhang, B. Xu, X. Wang, L. Gong, J. Chen, C. Hu, Y. Tong, J. Zhou, and Z. L. Wang, Flexible solid-state supercapacitors based on carbon nanobarticles/MnO_2 nanorods hybrid structure, *ACS Nano*, **6**

(2012) 656-661.

[20] K.-W. Park, H.-J. Ahn, and Y.-E. Sung, All-solid-state supercapacitor using a Nafion polymer membrane and its hybridization with a direct methanol fuel cell, *J .Power Sources*, **109** (2002) 500-506.

[21] C.-C. Yang, S.-T. Hsu, and W.-C. Chien, All solid-state electric double-layer capacitors based on alkaline polyvinyl alcohol polymer electrolytes, *J. Power Sources*, **152** (2005) 303-310.

[22] X. Liu, T. Momma, and T. Osaka, All-solid state electric double layer capacitor using polymer electrolyte and isotropic high density graphite electrodes, *Chem. Lett*., **8** (1996) 625-626.

[23] A. Matsuda, T. Kanzaki, Y. Kotani, M. Tatsumisago, and T. Minami, Proton conductivity and structure of phosphosilicate gels derived from tetraethoxysilane and phosphoric acid or triethylphosphate, *Solid State Ionics*, **139** (2001) 113-119.

[24] K. Tadanaga, H. Yoshida, A. Matsuda, T. Minami, and M. Tatsumisago, Preparation of proton-conductive inorganic-organic hybrid films from 3-glycidoxypropyltrimethoxysilane and orthophosphoric acid, *Chem. Matt.*, **15** (2003) 1910-1912.

[25] M. Aoki, K. Tadanaga, and M. Tatsumisago, All-solid-state electric double-layer

capacitor using ion conductive inorganic-organic hybrid membrane based on 3-glycidoxypropyltrimethoxysilane, *Electrochem. Solid-State Lett.* **13** (2010) A52-A54.

[26] A. Matsuda, H. Honjo, M. Tatsumisaga, and T. Minami, Proton conductive silica gels doped with several acids and their application to electric double-layer capacitor, *Chem. Lett.*, **11** (1998) 1189-1190.

[27]H. Gao, F. Xieo, C. B. Ching, and H. Duan, High-performance asymmetric supercapacitor based on graphene hydrogel and nanostructured MnO_2, *ACS Appl. Mater. Interfaces*, **4**, (2012) 2801-2810.

[28]M. S. Hong, S. H. Lee, and S. W. Kim, Use of KCl aqueous electrolyte for 2 V manganese oxide/activated carbon hybrid capacitor, *Electrochem. Solid-State Lett.* **5** (2002) A227-A230.

[29] X. Zhang, X sun, H. Zhang, D. Zhang, and Y. Ma, Development of redox deposition of birnessite-type MnO 2 on activated carbon as high-performance electrode for hybrid supercapacitors, *Mat. Chem. Phys*., **137** (2012) 290-296.

[30] Y.-C. Hsieh, K.-T. Lee, Y.-P. Lin, N.-L.-Wu, and S. W. Donne, Investigation on capacity fading of aqueous $MnO_2 \cdot nH_2O$ electrochemical capacitor, *J. Power*

Sources, **177** (2008) 660-664.

[31] W. Wei, X. Cui, W. Chen, and D. G. lvey, Electrochemical cyclability mechanism for MnO_2 electrodes utilized as electrochemical supercapacitors, *J. Power Sources*, **186** (2009) 543-550.

[32] T. Aoshima, K. Okahara, C. Kiyohara, and K. Shizuka, Mechanisms of manganese spinels dissolution and capacity fade at high temperature, *J. Power Sources*, **97-98** (2001) 377-380.

FIGURE CAPTIONS

Fig. 1. X-ray diffraction patterns of the (a)MnO_2, (b)CNT, and (c)MnO_2-CNT composite.

Fig. 2. SEM images of the (a)MnO_2, (b)CNT, and (c)MnO_2-CNT composite.

Fig. 3. Cyclic voltammograms of the (a)MnO_2, (b)CNT, and (c)MnO_2-CNT composite between 0 and 1.0 V (vs. Ag/AgCl) in 0.5 M Na_2SO_4 aqueous solution at the scan rate of 5 mV s^{-1}.

Fig. 4. Cyclic voltammograms of all-solid-state ECs at -30°C, 25°C, and 100°C at the scan rate of 50 mV s^{-1}.

Fig. 5. Galvanostatic charge-discharge curves of all-solid-state ECs at the operation temperatures of -30°C, 25°C, and 100°C at the current density of 1 mA cm^{-1}.

Fig.6. Specific discharge capacitance as a function of discharge current density for all-solid-state ECs at the operation temperatures of -30°C, 25°C, and 100°C.

Fig.7. Cycle performance of all-solid-state ECs at the operation temperatures of -30°C, 25°C, and 100°C.

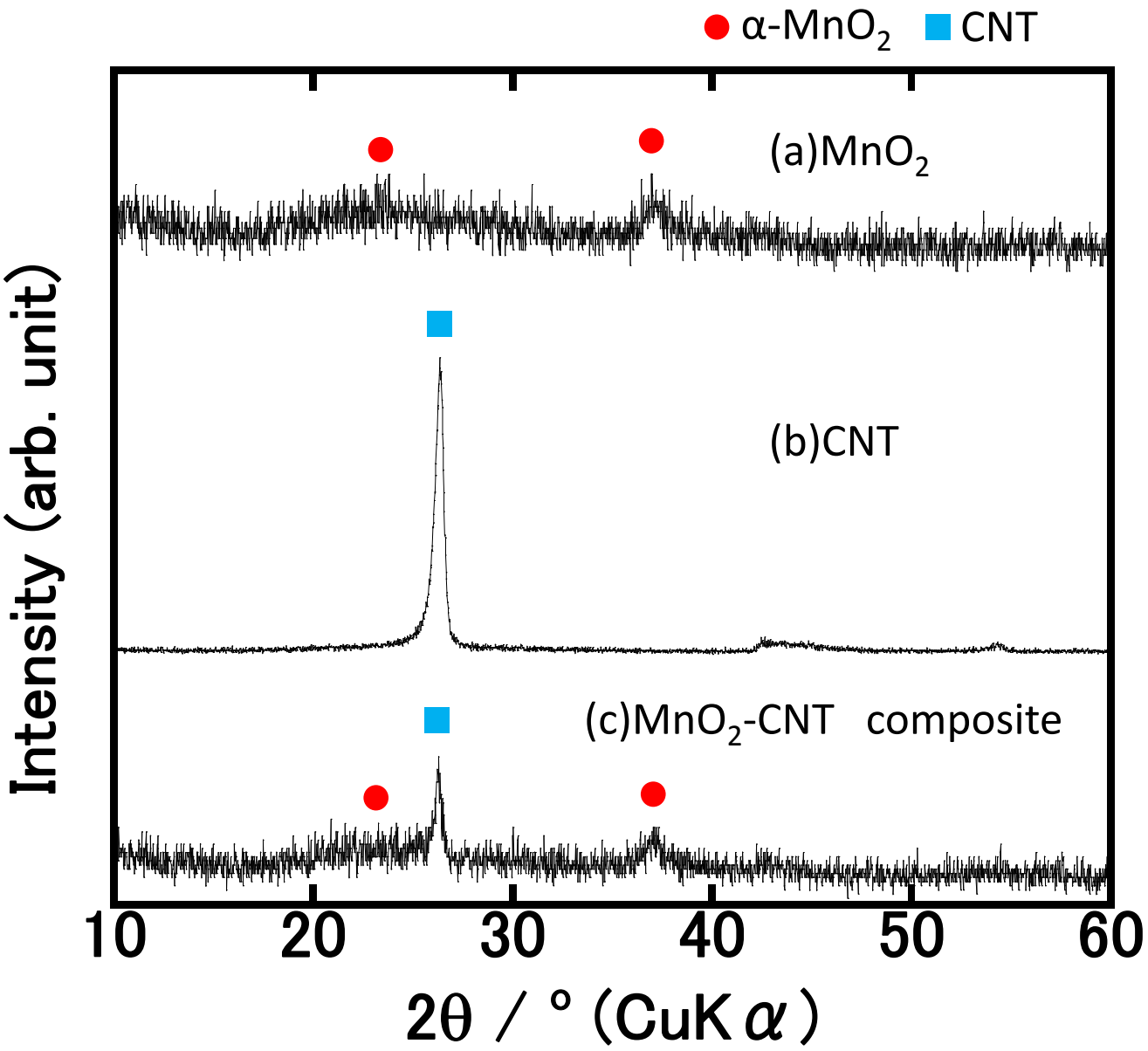
α-MnO2
CNT
(a)MnO2
(b)CNT
(c)MnO2-CNT composite
Intensity (arb. unit)
10
20
30
40
50
60
2θ / ° (CuKα)

Figure 1

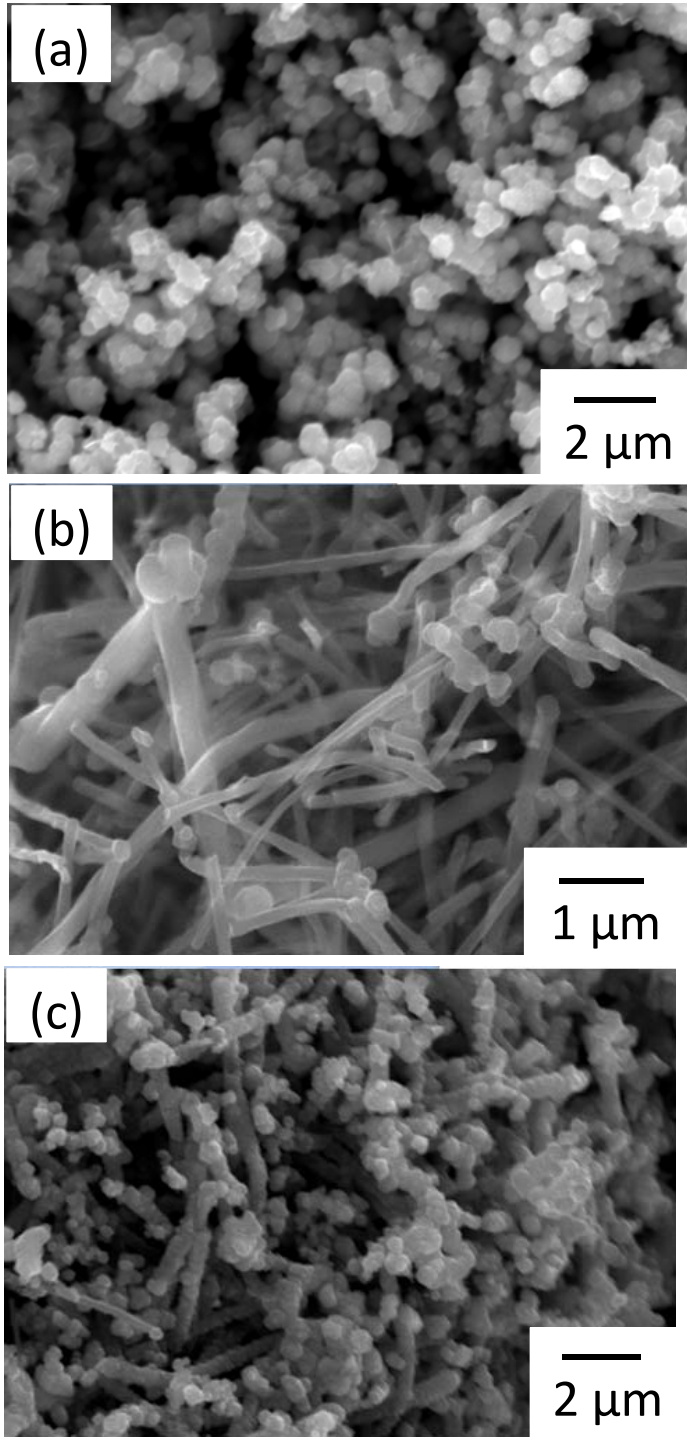

Figure 2

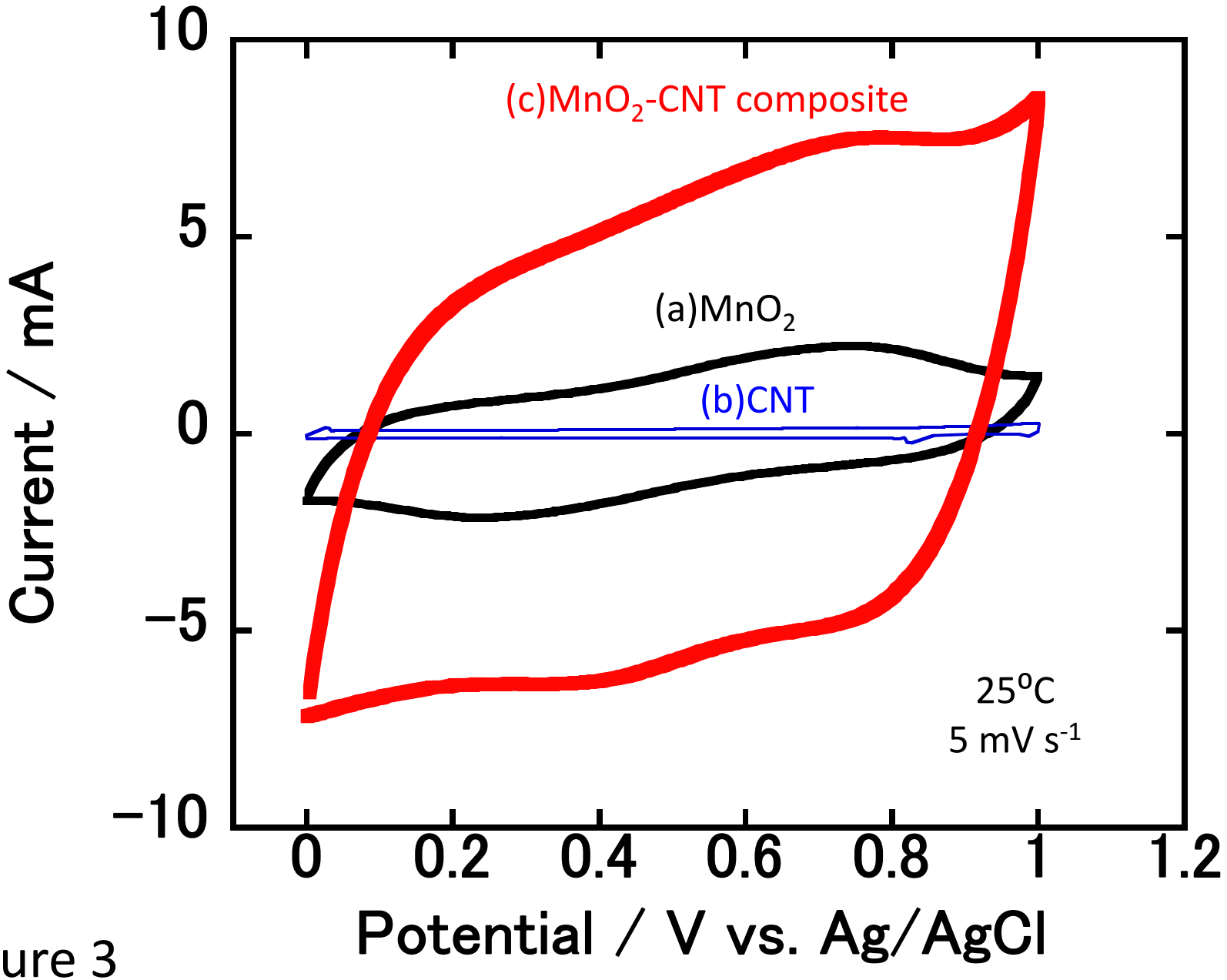
10
5
0
−5
−10
Current / mA
0
0.2
0.4
0.6
0.8
1
1.2
Potential / V vs. Ag/AgCl
(c)MnO2-CNT composite
(a)MnO2
(b)CNT
25°C
5 mV s-1

Figure 3

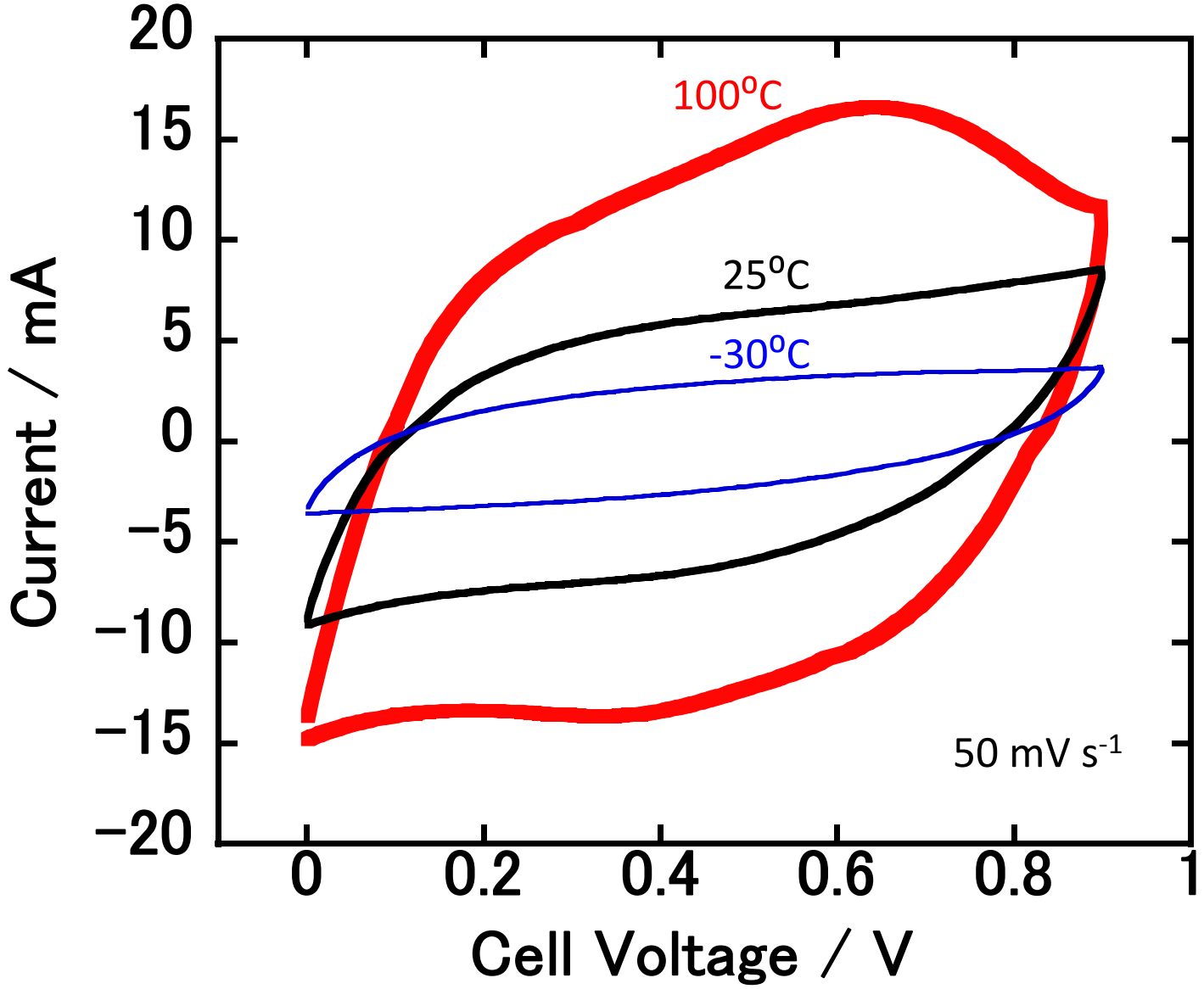
20
15
10
5
0
−5
−10
−15
−20
Current / mA
0
0.2
0.4
0.6
0.8
1
Cell Voltage / V
100°C
25°C
-30°C
50 mV s-1

Figure 4

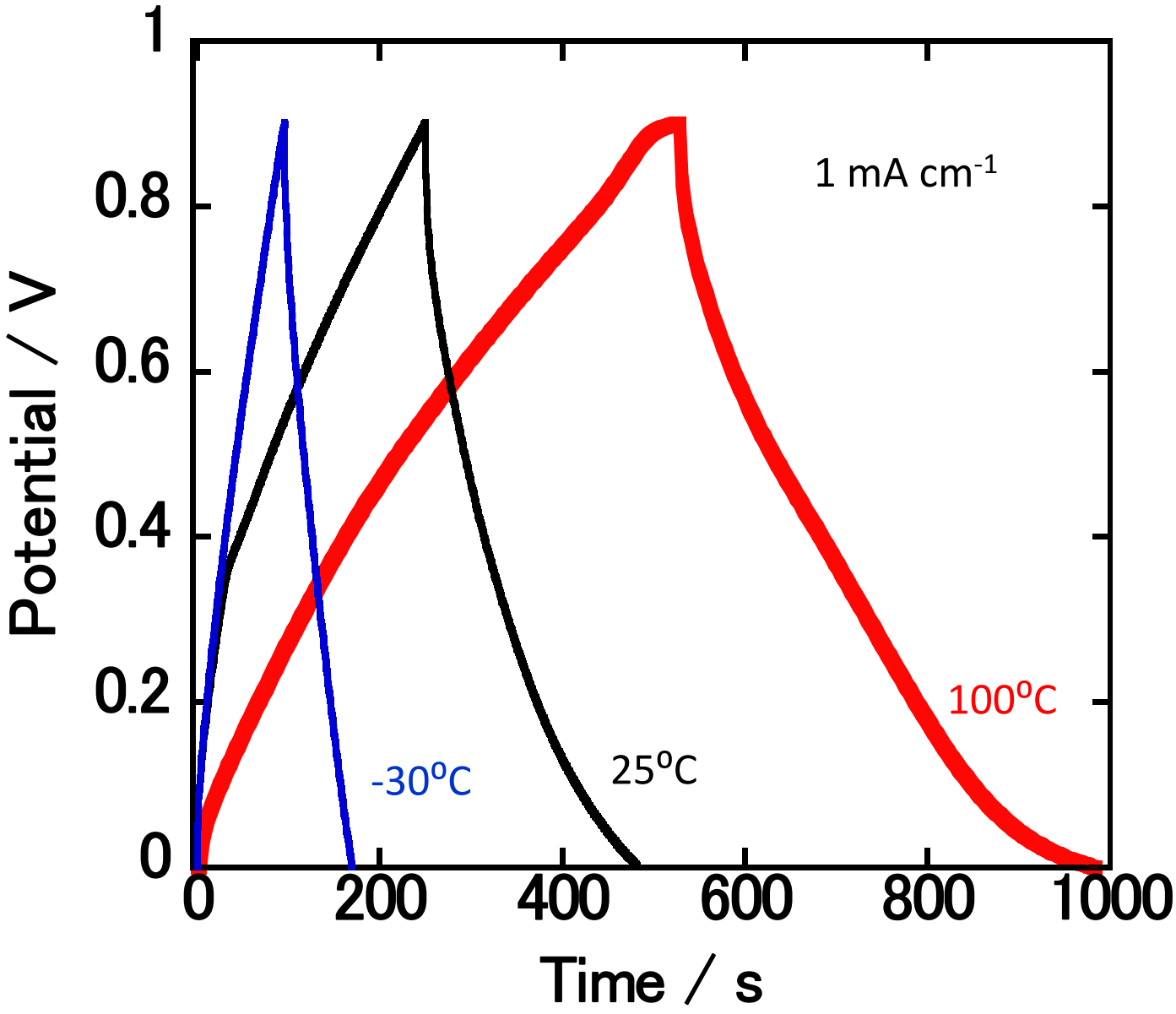
1
0.8
0.6
0.4
0.2
0
Potential / V
0
200
400
600
800
1000
Time / s
1 mA cm-1
-30°C
25°C
100°C

Figure 5

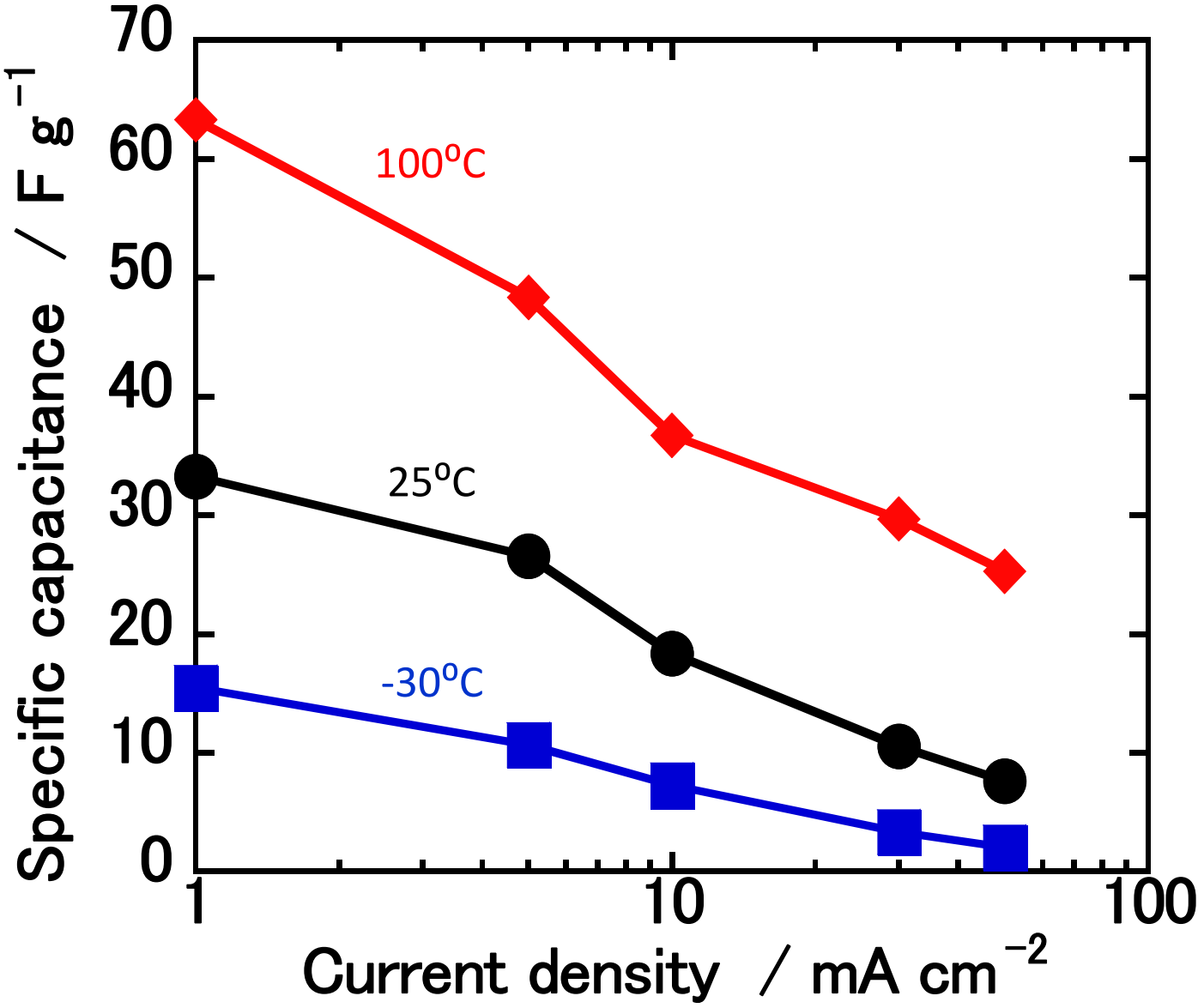
70
60
50
40
30
20
10
0
Specific capacitance / F g^{-1}
100°C
25°C
-30°C
1
10
100
Current density / mA cm^{-2}

Figure 6

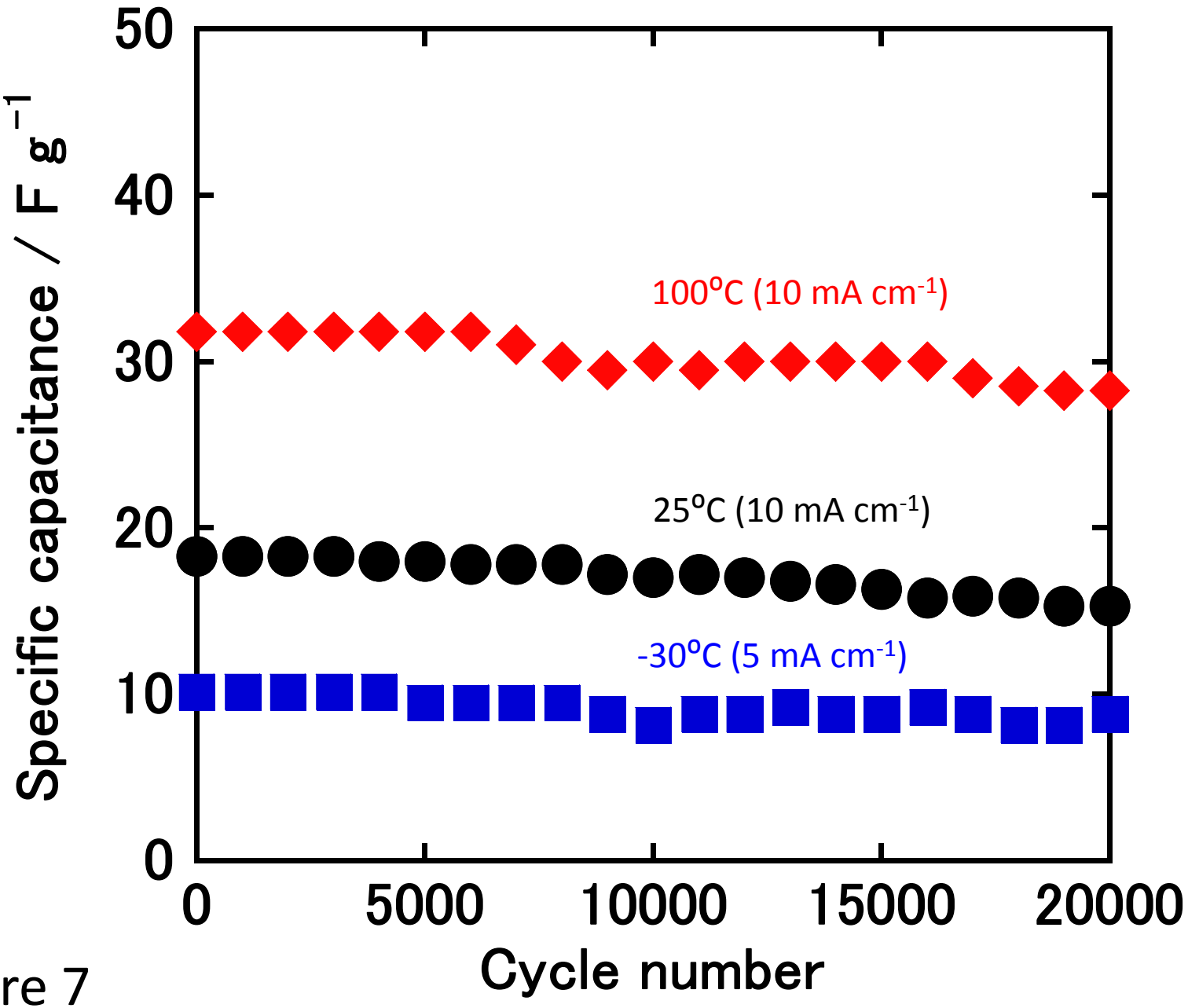
Specific capacitance / F g^{-1}
50
40
30
20
10
0
0
5000
10000
15000
20000
Cycle number
100°C (10 mA cm^{-1})
25°C (10 mA cm^{-1})
-30°C (5 mA cm^{-1})

Figure 7